Biotechnology and Bioprocess Engineering 16: 593-602 (2011)
DOI 10.1007/s12257-010-0348-9

RESEARCH PAPER

Mesenchymal Stem Cells on a Decellularized Cartilage Matrix for Cartilage Tissue Engineering

Xi-Fu Zheng, Shi-Bi Lu, Wei-Guo Zhang, Shu-Yun Liu, Jing-Xiang Huang, and Quan-Yi Guo

Received: 4 October 2010 / Revised: 26 November 2010 / Accepted: 30 November 2010

Abstract An ideal scaffold for cartilage tissue engineering should be biomimetic in not only its biochemical composition, but also in the morphological structure of the scaffold. In this study, we fabricated a scaffold with an oriented structure using a nanofibrous articular cartilage extracellular matrix (ACECM), in which the ACECM was used to mimic the biochemical composition and oriented structure of articular cartilage. Histology analysis showed that the scaffold contained cartilage ECM (GAGs and collagen II). Scanning electron microscopy (SEM) indicated that the scaffolds were composed of nanofibers and possessed vertical microtubules. Chondrogenic differentiation-induced mesenchymal stem cells (MSCs) were seeded on the scaffold *in vitro*. SEM showed that MSCs proliferated well and aligned along the vertical microtubules, which mimicked the orientation of deep zone articular cartilage. A cell proliferation assay and live/dead cell staining demonstrated that the ACECM possessed good cell affinity, which favored cell adherence and proliferation. The MSCs that had been labeled with the fluorescent dye PKH26 and seeded on scaffolds were implanted into nude mice. The differentiated cells/ACECM implants formed cartilage-like tissue 4 weeks after implantation, and stained positive for collagen type II and toluidine blue. In addition, the *in vivo* fluorescent images verified that the MSCs in the implants were the labeled MSCs. These results demonstrated that the oriented ACECM scaffolds hold great promise for use in cartilage tissue engineering applications.

Keywords: biomimetic material, oriented scaffold, decellularization, nanofiber, cartilage tissue engineering

Xi-Fu Zheng, Wei-Guo Zhang
Department of Orthopedic Surgery, First Affiliated Hospital, Dalian Medical University, Dalian 116-011, China

Xi-Fu Zheng, Shi-Bi Lu, Shu-Yun Liu, Jing-Xiang Huang, Quan-Yi Guo*
Institute of Orthopedics of Chinese PLA, Chinese PLA General Hospital, Beijing 100-853, China
Tel: +86-10-6693-6637; Fax: +86-10-6693-9205
E-mail: guoquanyi301@gmail.com

1. Introduction

Cartilage repair is a significant challenge for modern orthopedic surgery due to the limited regeneration ability of mature articular cartilage in various joint injuries, such as trauma or arthritis [1]. Promising tissue engineering technology provides more advantages compared with the traditional treatment strategies for cartilage repair [2,3]. For cartilage tissue engineering, the natural polymers extracted from the extracellular matrix (ECM) such as collagen, hyaluronic acid and fibrin, as well as synthetic polymers such as PGA, PLA and their co-polymers PLGA have been developed and applied widely [4-8].

Synthetic polymers have good mechanical properties, satisfactory biocompatibility and controlled biodegradation rates. However, their surfaces have low intrinsic bioactivity and are hydrophobic; thus, these materials are not recognized by cell-surface receptors [9]. Moreover, the acidic degradation products of some synthetic polymers, such as PLGA, may induce inflammatory responses [10,11]. Natural polymers are functional and bioactive when compared with synthetic polymers, because they provide informational signals, which facilitate cell attachment, proliferation and differentiation. However, the native ECM is complex and multi-factorial, which can provide an optimal microenvironment for cell seeding, adherence and proliferation. Thus, it is exceedingly difficult to mimic native ECM microenvironments using a single extract.

As a new method to obtain native ECM, the decellulari-

zation technique has been used to effectively remove cellular antigens and nuclear materials while minimizing adverse effects on composition and biological activity of the remaining ECM [12]. The development of ECM scaffolds using a variety of decellularized tissues, including heart valves, blood vessels, skin and nerves have been studied for tissue engineering and regenerative medicine applications [13-16]. However, little work has been conducted to explore decellularized articular cartilage for the fabrication of porous scaffolds. The cartilage is compact and hard and chondrocytes were encapsulated in the surrounding ECM. Therefore, it is difficult to obtain decellularized articular cartilage extracellular matrix (ACECM).

The primary goal of tissue engineering is to regain the structure and function of the original tissue. Thus, it is highly important that the morphological structure of the scaffold acts as a biomimetic of the native tissue [17-19]. In addition, the organization of the articular cartilage collagen network has been shown to display zonal variations and the orientation of collagen fibers in the deep zone cartilage is vertical to the subchondral bone. This spatial organization can impact chondrocytes orientation and proliferation. Therefore, an oriented scaffold loaded with cells will mimic the structure of articular cartilage.

In this study, a nanofibrous ACECM was fabricated using a physical and chemical decellularization procedure and a porous oriented scaffold was produced using an improved thermal induced phase separation (TIPS) technique. To verify the feasibility of this novel scaffold for cartilage regeneration, the morphology of the scaffold was imaged by scanning electron microscopy (SEM), the biochemical components were detected by histology staining, cell affinity and orientation on the scaffold were evaluated *in vitro* and the ability of the scaffold to support cartilage formation was investigated by seeding PKH26 labeled MSCs *in vivo*.

2. Materials and Methods

2.1. Preparation of ACECM oriented scaffold

2.1.1. Pulverization and decellularization of articular cartilage

An improved method for decellularization was developed based on a previously published method [20]. Porcine knee joints were obtained from the abattoir immediately after slaughter, covered with ice bag and transported to laboratory. Cartilage slices were cut from femoral condyles under aseptic conditions. The cartilage was decellularized using both physical and chemical procedures as follows. The slices were suspended and rinsed in sterile PBS solution three times, then homogenized under a powerful shearing force using a tissue disintegrator to form a suspension slurry and centrifugated using the differential centrifugation method. The suspension was centrifugated in a centrifuge (Beckman Allegra X-22R, USA) for 5 min at 1,500 revolutions per minute (rpm) with a F0850 rotor. The suspended microparticles were separated with precipitated macroparticles. The suspended microparticles were centrifuged for another 5 min at 3,000 rpm and 20 min at 6,000 rpm successively. The suspended cartilage microparticles were centrifugated again for 35 min at 9,500 rpm and the fibrous precipitated ACECM were collected. The precipitate was rinsed and centrifuged twice at 9,500 rpm with sterile PBS solution. The ACECM precipitate was digested in 3% TritonX-100 and 0.25% trypsin (containing 0.1% EDTA, 0.1% sodium azide) successively with gentle agitation for 12 h at 4ºC, then 12 h in 50 U/mL deoxyribonuclease I and 1 U/mL ribonuclease A (Sigma, St. Louis, MO, USA) with agitation at 37ºC to remove nuclear materials after being washed in PBS without protease inhibition. After decellularization, the ACECM precipitation was again centrifugated at 9,500 rpm. All the nanofibrous ACECM precipitate were stored in sterile glassware for fabrication of the scaffolds.

2.1.2. Fabrication of ACECM oriented scaffold

The reserved nanofibrous ACECM was washed twice with sterile PBS and diluted to a predetermined concentration of 5% (w/w). The procedure used to fabricate the oriented scaffold was as follows. After the ACECM was infused into a 4 or 8 mm cylindrical mould, the mould was placed vertically onto a metal plate in a refrigerator maintained at –20ºC and frozen for a half hour. After the mould was completely frozen, it was placed into a refrigerator maintained at –20ºC for another 2 h. The mould was then transferred into a freezer dryer and lyophilized for 48 h under vacuum. The ACECM scaffolds were removed from the mould and cross-linked by ultraviolet light at a wavelength of 258 nm for 4 h. The scaffolds were immersed into a 95% (v/v) alcohol solution (containing 50 mM 1-ethyl-3-(3-dimethylaminopropyl) carbodiimide hydrochloride [EDAC] and 20 mM N-hydroxysucinimide [NHS]; Sigma, St. Louis, MO, USA) for 24 h at 4ºC. Excess EDAC was rinsed from the scaffolds by PBS repeatedly. ACECM oriented scaffolds approximately 4 or 8 mm in diameter were fabricated. The scaffolds were sterilized by ethylene oxide and prepared for use.

2.2. Evaluation of nanofibrous ACECM and oriented scaffold

2.2.1. Microstructure of nanofibrous ACECM

To observe the morphology and size of the nanofibrous ACECM, the ACECM precipitates were diluted to 3% (w/w) and smeared onto a microscopic slide. The ACECM was then dehydrated through a series of graded alcohols and dried at room temperature. The samples were sputter-coated with gold and observed by SEM (Hitachi BCPCAS-4800, Tokyo, Japan).

2.2.2. Characterization of the oriented scaffold

The scaffold was coated with gold using a sputter coater (Denton Vacuum Desk-II, Moorestown, USA). The morphology of the scaffold was observed by SEM (JEOL JSM-6700F, Tokyo, Japan). The diameter of the scaffold microtubules was calculated based on the SEM micrographs at a magnification of × 100. For each scaffold, the average diameter of the microtubules was calculated from 50 different microtubules.

The porosity of the scaffolds was measured by liquid displacement as described previously with slight modifications [21]. Briefly, scaffolds were cut into 4 × 4 × 1 mm pieces, placed in a 10 mL cylinder containing a defined volume of ethanol (V1) and then pressed to force all trapped air out of the scaffold. The total volume of ethanol and the ethanol-impregnated scaffold was recorded as V2. The ethanol-impregnated scaffold was removed from the cylinder and the residual ethanol volume was recorded (V3). The porosity of the scaffold was expressed as:

$$\text{Porosity} = (V1 - V3) / (V2 - V3).$$

2.2.3. Histological and immunohistochemical assay of scaffold

The scaffolds were mounted using the O.C.T. compound (Tissue-Tek, Miles, USA). Cryosections (10 μm thick) were cut and fixed in acetone for 30 min at room temperature and slightly washed with PBS. The samples were assayed by safranin O staining for identifying the presence of cartilage derived glycosaminoglycans (GAGs).

The type II collagen was stained using a rabbit anti-collagen-II polyclonal antibody according to the manufactures' instruction. The cross and vertical sections were blocked with peroxidase blocking solution for 10 min and then 10% (v/v) goat serum solution for 30 min. The sections were incubated with anti-type II collagen (1:100 working dilution) overnight at 4ºC. A biotinylated secondary antibody (anti-rabbit FITC-conjugated immunoglobulins; Shiankexing, Beijing, China) was then applied for 30 min followed by incubation with horseradish peroxide-conjugated streptavidin for 10 min. Color was developed with diaminobenzidine tetrahydrochloride (DAB). Images were acquired by microscopy.

2.3. Isolation, culture, and chondrogenic induction of MSCs

With approval from the institutional review board of the Chinese PLA general hospital, mature New Zealand White rabbits (weight 2.5 ~ 3.0 kg) were anaesthetized. Mesenchymal stem cells (MSCs) were isolated and cultured as previously described [22]. P3 cells were used in these experiments. MSCs were resuspended in chondrogenic differentiation induced medium, which will be referred to as DMEM, supplemented with 0.1 mM ascorbic acid 2-phosphate, 40 μg/mL hydroxyproline, 10^{-7} M dexamethasone and 10 ng/mL TGF-β1, 25 ng/mL basic fibroblast growth factor (bFGF), and 1% ITS (10 μg/mL insulin, 5.5 μg/mL transferrin, 5 ng/mL selenium, 0.5 mg/mL bovine serum albumin, 4.7 mg/mL linoleic acid; Sigma, St. Louis, MO, USA). Medium was regularly changed every 2 days up to 21 days. Cells were harvested and used in the following experiments.

2.4. Seeding and morphology observation of cells

The cells were suspended in culture medium. The oriented scaffolds (4 mm diameter, 1 mm thickness) were placed into a 24-well culture plate and 20 μL of the cell suspension, which corresponded to approximately 1×10^5 cells, was seeded onto each sample until the scaffold became completely saturated. The scaffolds were cultured in a 5% CO_2 humidified atmosphere at 37ºC 4 h to allow for cell adherence, and then 2 mL of culture medium was added to each well. After the cells were cultured on the scaffolds for 3 and 7 days, the samples were washed with PBS and fixed with 2.5% glutaraldehyde for 24 h at 4ºC. The scaffolds were then dehydrated through a series of graded alcohols and dried at room temperature, the samples were sputter-coated with gold and cells in the samples were observed by SEM.

2.5. Cell proliferation assay

Cell proliferation was quantitatively evaluated using the cell counting kit-8 (Dojindo CCK-8 kit, Tokyo, Japan), which is a colorimetric method for determining the number of viable cells in culture. The oriented scaffolds were placed into a 24-well culture plate and 15 μL of the cell suspension, which contained approximately 5×10^4 cells, was seeded onto the top surface of the scaffold (4 mm diameter, 1 mm thickness) and allowed to penetrate into scaffold. The cells/scaffold structures were then incubated at 37ºC under 5% CO_2 for 4 h to allow for cells adherence. The structures were then transferred to a new 24-well plate and cultured in medium for additional 1, 3, and 7 days. At every indicated time interval, culture medium was discarded and approximately 500 mL of serum-free DMEM

medium with 50 μL CCK-8 solution were added to each sample, followed by incubation at 37ºC for 3 h. The supernatant was transferred to a 96-well plate and the optical density (OD) at 450 nm was measured using a microplate reader (Beckman, Fullerton, CA).

2.6. Cell viability assay

Cell viability in the cells/scaffold structures was evaluated after 3 and 7 days of culture using a Live/Dead assay kit (Sigma, St. Louis, MO, USA) according to the manufactures' instruction. Media was aspirated from the cultures and the structures were washed in PBS. The samples were then incubated in 5×10^{-3} mg/mL FDA for 5 min at 37ºC in the dark. The FDA was aspirated and structures were washed twice in PBS. The structures were incubated in a 5×10^{-3} mg/mL PI working solution for another 5 min. The PI solution was then aspirated and the structures were washed twice with PBS before being viewed with an Olympus IX81 confocal microscope (Olympus, Tokyo, Japan).

2.7. Cells labeling

Chondrogenic induced MSCs were labeled with fluorescent dye PKH26 (Sigma, St. Louis, MO, USA) as follows. Induced MSCs were digested with trypsin, then counted and washed in serum-free medium. The MSCs were centrifuged and suspended in 1 mL of dilution buffer provided in the manufacturer's labeling kit. The MSCs suspension was mixed with an equal volume of the labeling solution containing 4×10^{-6} M PKH26 in dilution buffer and incubated for 5 min at room temperature. The label reaction was terminated by adding 2 mL of FBS. The MSCs were washed two times with 10% FBS DMEM and centrifuged.

2.8. Preparation and implantation

The cells were suspended in chondrogenic differentiation-induced medium. The sterilized oriented scaffolds (4 mm diameter, 3 mm thickness) were placed into a 24-well culture plate and 50 μL of the cell suspension, which corresponded to approximately 2×10^6 cells, was seeded onto each sample until the scaffold became completely saturated. The cells were cultured with the scaffold structures were under a 5% CO_2 humidified atmosphere at 37ºC for 4 h to allow for cells adherence, and then 2 mL of culture medium was added to each well. The structures were observed under a fluorescent microscope and then cultured in medium. The animal experiment was conducted according to the committee guidelines for animal experiments of the laboratory animal research centre, at Chinese PLA general hospital. After *in vitro* culture for 3 days, the structures were implanted subcutaneously in the dorsa of nude mice (n = 4). Four weeks after implantation, the implants were detected using a fluorescent imaging system.

2.9. Fluorescent imaging

The implants were imaged using an *In-vivo* Imaging System FX (Kodak Jingmei Biotech, Beijing, China). After anesthetization with 80 mg/kg ketamine, the nude mice were placed into the imaging cabinet and imaged at an excitation and emission wavelength of 450 ~ 570 nm and 570 ~ 700 nm respective. The other imaging parameters were as follows: exposure time, 1 min; F-stop, 4.0; FOV, 100 mm; resolution, 650 dpi; and optical density 0.5. At the end of experiment, the mice were sacrificed and implants were harvested.

2.10. Histology and immunohistochemistry

The implants were fixed in 4% phosphate-buffered paraformaldehyde, dehydrated through a graded series of ethanol, embedded in paraffin, sectioned at a thickness of 10 μm and evaluated by staining with toluidine blue and immunohistochemically with type II collagen.

2.11. Statistical analysis

The results of the CCK-8 experiments were expressed as the mean ± standard deviation and assessed by one way analysis of variance (ANOVA). Comparison between two means was analyzed using the Tukey's test, where $p < 0.05$ was considered statistically significant.

3. Results

3.1. Characterization of nanofibrous ACECM

The morphology and diameter of ACECM fibers were observed by SEM (Figs. 1A and 1B). The decellularized ACECM had a fibrous shape and were on the nanometer scale. The diameter of the nanofibrous ACECM was approximately 50 nm. The nanofibrous and oriented structure characteristics of the scaffold are displayed in Figs. 1C and 1D. In the cross section image of the scaffold, the nanofibrous ACECM were shown to be aligned randomly (Fig. 1C) and some nanofibers were connected in the pore space. Fig. 1D shows that the nanofibrous ACECM was aligned along the vertical orientation.

3.2. Characterization of the oriented scaffold

To analyze the biochemical composition of the oriented scaffold, histological and immunofluorescent staining was conducted. Immunofluorescent staining revealed the presence of collagen II (Figs. 2A and 2C), while safranin O positive staining indicated that GAGs were present in the oriented scaffold (Figs. 2B and 2D). The vertical section of the scaffold indicated the vertical microtubule structure.

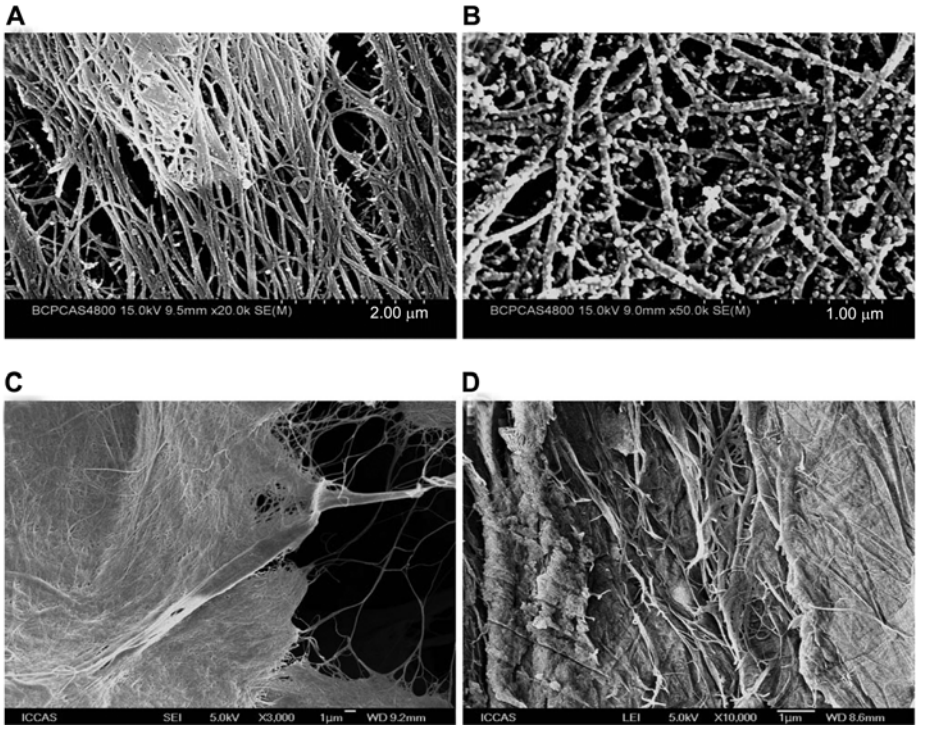

Fig. 1. The morphology and diameter of the ACECM and the wall of the oriented scaffold were observed by SEM. (A, B) The ACECM adopted a fibrous shape and random alignment and was on the nanometer scale. (C) In the cross section image of the scaffold wall, the nanofibrous ACECM was shown to be interconnected and aligned randomly. (D) The nanofibrous ACECM aligned along vertical orientation in vertical section. (A) Bar = 2 μm. (B, C, and D) Bar = 1 μm.

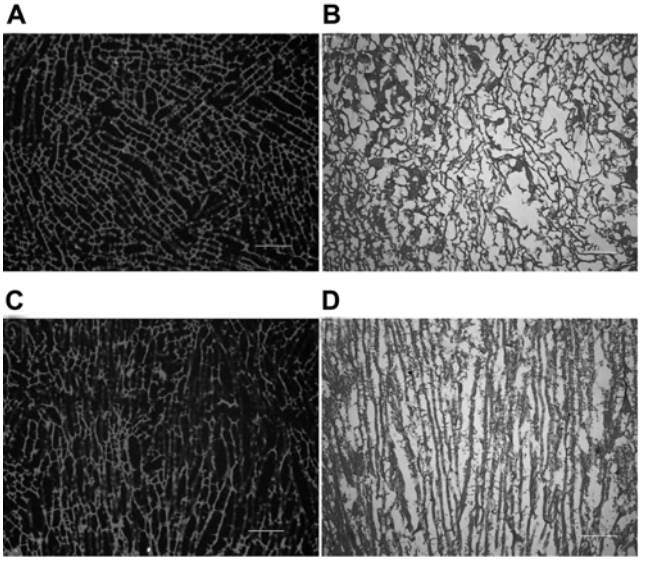

Fig. 2. Histological and immunohistochemical staining of the ACECM oriented scaffold. (A, C) Immunofluorescent positive staining indicated that collagen II was present in the oriented scaffold. (B, D) Safranin O staining revealed the presence of GAGs. Bar = 200 μm.

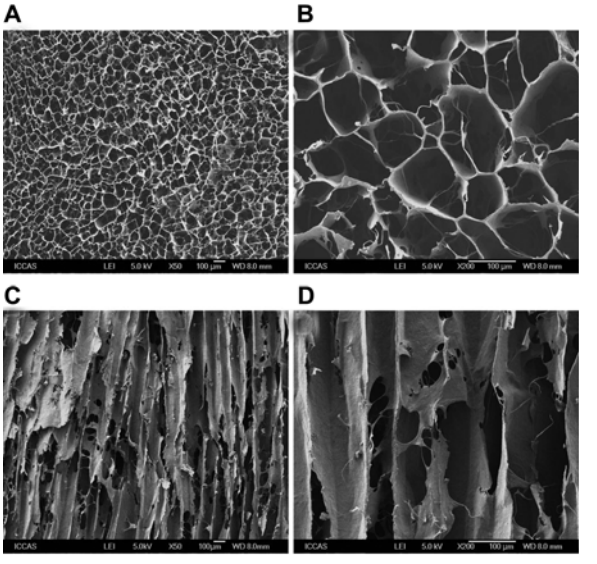

Fig. 3. The microstructure of the ACECM oriented scaffolds was examined by SEM. (A, C) The porous structures were interconnected homogeneously and distributed uniformly in the cross section image of the oriented scaffold. (B, D) The vertical microtubules were oriented and interconnected congruously in the vertical section. Bar = 100 μm.

Fig. 3 shows the microstructure of the ACECM oriented scaffolds. The SEM images (Figs. 3A and 3C) shows the cross section of the oriented scaffold. Based on these images, the oriented ACECM scaffold was shown to have a homogeneous interconnected porous structure and the pores were distributed uniformly. Figs. 3B and 3D show the structure of the scaffold in the vertical orientation. The

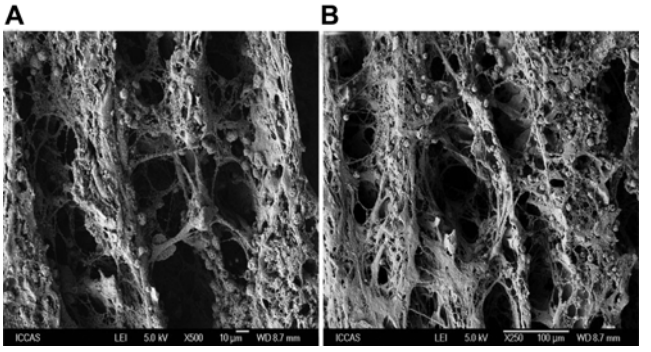

Fig. 4. SEM micrographs of MSCs adhered on the oriented scaffolds. (A) The MSCs adhered and were aligned vertically along the oriented microtubules after 3 days of culture. (B) More cells were spread and aligned along the vertical microtubules, aggregated with each other and filled the pores of the scaffold after 7 days of culture. (A) Bar = 10 μm. (B) Bar = 100 μm.

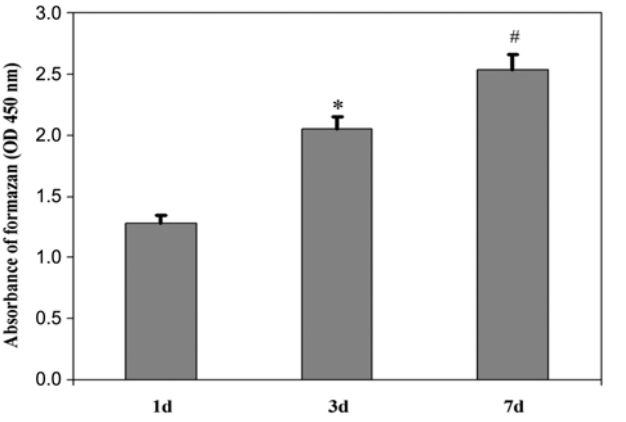

Fig. 5. Proliferation of MSCs on the scaffolds was measured using the CCK-8 quantitative assay. n = 6. (*)$p < 0.05$ and ($^{\#}$)$p < 0.05$. In comparison with 1 and 3 days respectively of cell proliferation on the oriented scaffold. The results indicated that the ACECM scaffold possessed good cell affinity.

vertical microtubules were interconnected and congruously aligned. Some micropores were present in the wall of the vertical microtubules. The vertical microtubules in the oriented scaffold mimicked the deep zone articular cartilage. The scaffold porosity and pore diameter was 91.3% and 104 ± 30 μm, respectively.

3.3. Cell morphology and alignment on oriented scaffold

Fig. 4 shows the morphology of the MSCs adhered on the scaffold after 3 ~ 7 days of culture. After 3 days, the cells had adhered onto the oriented scaffold and were distributed within the pores; most cells adopted an ellipse or spindle shape, were aligned vertically along the oriented microtubules and covered the pore space, which indicated that the cells proliferated well on the scaffold (Fig. 4A). After 7 days of culture more cells had were adhered to the scaffold when compared to 3 days of culture. The cells spread along the vertical microtubules, aggregated with each other and filled the pore space (Fig. 4B), which could form an oriented neo-tissue.

3.4. Cell proliferation and viability on oriented scaffold

The proliferation of MSCs on scaffold was assessed using the CCK-8 quantitative assay after 1, 3, and 7 days of culture (Fig. 5). The results of this assay demonstrated that the MSCs proliferated rapidly and were viable on the oriented scaffold. Thus, the ACECM had good compatibility and cellular affinity. The cells status and viability are shown in Fig. 6. On day 3, there were many live cells (green spots) adhered on the scaffold and only a few dead cells (red spots) were dispersed sporadicly throughout the scaffold. At longer culture times, more green spots were aligned along the oriented microtubules and only a few red spots were observed after 7 days of culture (Figs. 6A and 6B). This indicated that the cells rapidly proliferated and

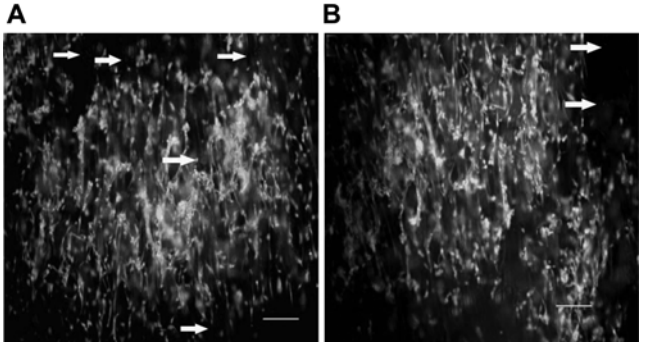

Fig. 6. Live/dead cells staining of MSCs cultured on the scaffold for 3 days (A) and 7 days (B). (A) Live cells were numerous and aligned vertically along the microtubules, while only a few dead cells were dispersed throughout the scaffold. (B) The number of live cells increased and the number of dead cells decreased. Arrows represent the dead cells. Bar = 200 μm.

the scaffold possessed good cell affinity. The oriented alignment and viability of adhered cells were in agreement with the results of the SEM micrographs and CCK-8 assay.

3.5. Cell labeling and tracking *in vivo*

The PKH26 concentration tested was sufficient for labeling the chondrogenic differentiation-induced MSCs. As shown in Fig. 7, the labeled cells (red fluorescence) were distributed uniformly in the center and edge of the scaffold. Four weeks after implantation, the cells-scaffold structures in the nude mice were imaged using the *in vivo* imaging system. An X-ray image of the nude mice is shown in Fig. 8A, which was used to locate the implanted scaffold. The red fluorescence of the PKH26 labeled MSCs-scaffold implants was observed in Fig. 8B. Fig. 8C is an overlay the images shown in A and B and clearly demonstrates that the implant was situated in the dorsa of the nude mice. Using the intensity ruler, the implant was shown to emit hyper-

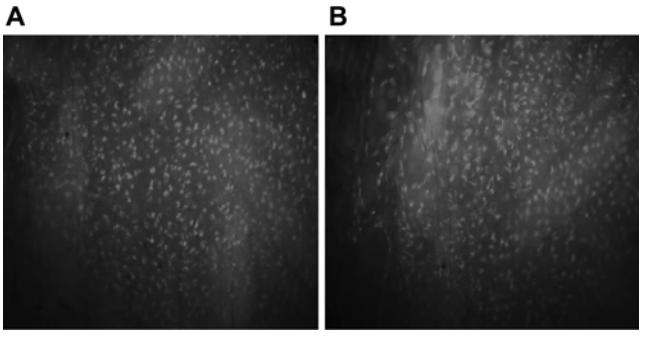

Fig. 7. The MSCs labeled with PKH26 were distributed uniformly in the center (A) and edge (B) of the scaffold. Magnication × 200.

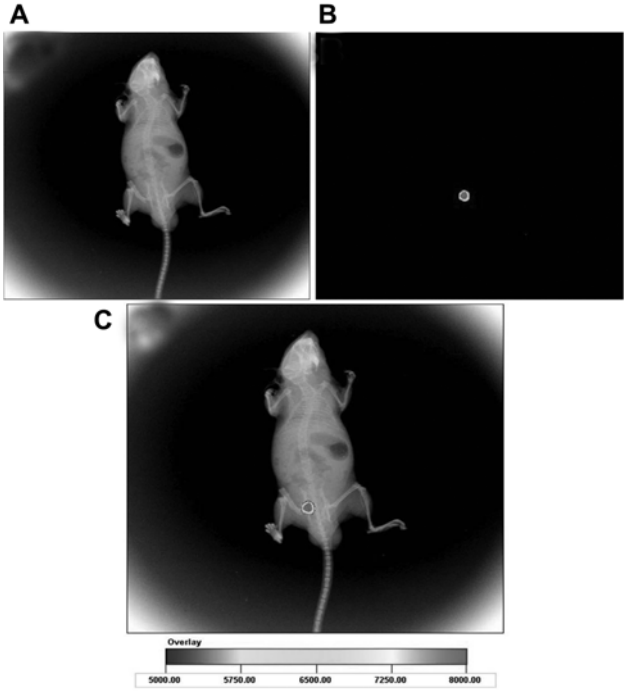

Fig. 8. The PKH26 labeled MSC-ACECM scaffold structures in nude mice were imaged using the *in vivo* fluorescent imaging system. (A) X-ray imaging of nude mice. (B) The red fluorescence of labeled MSCs-scaffold structures. (C) Overlay of the images shown in A and B, which clearly demonstrated that the implant was situated in dorsa of the nude mice.

fluorescence. The fluorescent imaging demonstrated that the implants contained the PKH26 labeled chondrogenic differentiation-induced MSCs-ACECM scaffold structures.

3.6. Histological and immunohistochemical staining

Toluidine blue and immunohistochemical staining of the implants are shown in Fig. 9. The toluidine blue staining indicated the presence of secreted ECM in the GAGs and round chondrocyte-like cells were surrounded by an abundant ECM (Figs. 9A and 9C). The results of collagen II immunohistochemistry (Figs. 9B and 9D) demonstrated that the implanted cells secreted collagen II in the micro-

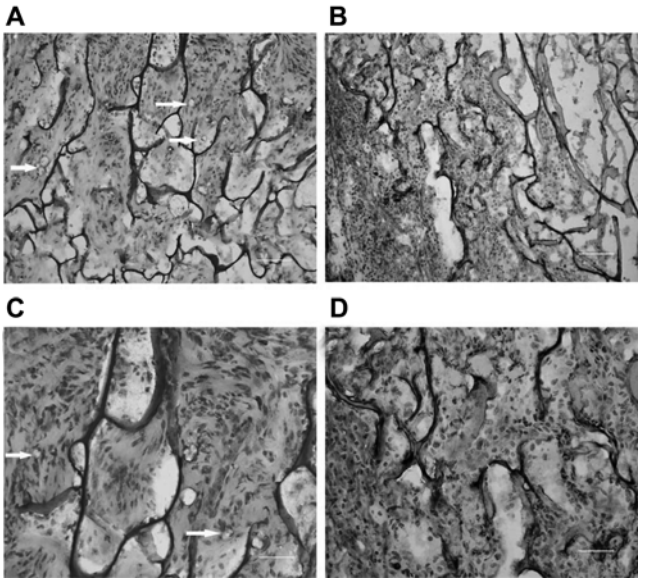

Fig. 9. The implants were stained by histology and immunohistochemistry. (A, C) Toluidine blue staining indicated the presence of chondrocyte-like cells and secreted ECM rich in GAGs. (B, D) The positive immunohistochemistry results indicated that the implanted MSCs secreted collagen II in the microenvironment of the ACECM. Arrows represent the lacunae structures. (A, B) Bar = 100 μm. (C, D) Bar = 50 μm.

environment of ACECM *in vivo*. The staining results showed that the chondrocyte-like cells proliferated and secreted ECM. In addition, the ACECM retained the phenotype of differentiated stem cells and MSCs-scaffold structure formed the appropriate tissue engineering cartilage in the ACECM microenvironment *in vivo*.

4. Discussion

The ideal cartilage scaffold should mimic the ECM composition and morphological structure of the cartilage, which is good for cells adherence and alignment. In this study, a nanofibrous ACECM derived oriented scaffold was fabricated. SEM showed that MSCs proliferated well and were aligned along the vertical microtubules of the scaffold. The cell proliferation assay and live/dead cells staining showed the ACECM had a high cell affinity. The *in vivo* evaluation, histological examination and immunohistochemical staining of the implants were all positive for chondrogenic differentiation. These results imply that the ACECM oriented scaffolds have good biocompatibility with differentiated MSCs and strongly mimic the deep zone of articular cartilage. In addition, the ACECM was shown to provide and excellent microenvironment for MSCs adhesion, proliferation and chondrogenic differentiation.

One objective of this study was to fabricate a nanofibrous

ACECM oriented scaffold. However, it was difficult to shatter the cartilage and achieve effective penetration of the solutions used in the decellularization procedure. To obtain more decellularized cartilage, a novel method was used to obtain the nanofibrous ACECM in this study. The cartilage slices could absorb water sufficiently and become soft under moist conditions, which promoted permeation of chemicals and enzymes. Using this novel approach, nanofibrous ACECM was easily fabricated and collected (Fig. 1). In particular, the native cartilage ECM (GAGs and collagen II) was nanofibers. Furthermore, structures on the nanometer scale are known to be advantageous for cells adherence and proliferation, and can act as potent effectors of differentiation [23,24]. Here, we fabricated a nanofibrous ACECM from native articular cartilage (Fig. 1). Histological analysis showed that the ACECM oriented scaffold contained GAGs and collagen II (Fig. 2). These results demonstrated that the cartilage ECM remained after the decellularization process and chemical cross linking. Thus, the nanofibrous ACECM was a biomimetic of native cartilage ECM.

Using the traditional TIPS technique, scaffolds with high porosity and round-shape porous structure could be fabricated and have been widely used in tissue engineering applications [25,26]. The solid liquid phase separation process of traditional TIPS is due to the crystallization of solvent. The spherical crystals are produced by the crystal nucleus, which then grows in all directions. So, the porous structures were randomly aligned. To develop a scaffold that mimics the orientation of the deep zone cartilage, porous oriented scaffold with vertical microtubules could be fabricated using improved TIPS. The oriented scaffold could be manufactured by temperature gradient guided TIPS [27]. Therefore, by using a temperature gradient during phase separation, fibrous crystals were produced due to the growth of crystals along the direction of the temperature gradient. Using this approach, an oriented scaffold with vertical microtubules could be fabricated after freeze drying (Fig. 3). The pore size, porosity and pore structure of the scaffolds are important for cell adherence and proliferation. Thus, further studies should be conducted to examine the effect of different temperature gradients on pore size and the oriented structure of the ACECM scaffold.

The advantage of decellularization relies on signals present in the decellularized ECM, which promote cell adherence or facilitate the proliferation of seeded cells. In this study, the CCK-8 assay and cell viability staining showed that the adhered MSCs proliferated rapidly with time (Figs. 5 and 6). These results demonstrate that the ACECM possesses good cell affinity and provides a biomimetic ECM microenvironment for adhesion and proliferation of chondrogenic induced MSCs. Furthermore, the interconnected oriented structure promoted cell migration because the vertical microtubules could facilitate cellular infiltration into the pores and culture medium and nutrients could be easily exchanged through the oriented microtubules. Several *in vitro* studies have shown that the orientation of the scaffold can effect cell proliferation and orientation [28,29]. In this study, when cells were seeded on the oriented scaffold, the vertical microtubules could direct the alignment of adhered cells along the microtubules. The MSCs were aligned vertically along the microtubules and distributed throughout most of the pores (Fig. 4). The MSCs-oriented scaffold structures were a biomimetic of the deep zone cartilage and could form regenerated cartilage.

PKH26 has been widely used to track cells. The PKH26 fluorescence can persist for more than 4 weeks *in vivo*, and the fluorescence intensity can be used as an indirect measure of proliferation [30,31]. In this study, PKH26 was used to track cells in vivo and evaluate cell proliferation. Four weeks after implantation, hyperfluorescence was observed in the implants, indicating that the MSCs proliferated well (Fig. 8). The results of toluidine blue and collagen II staining of implants were positive, which indicated that the ACECM retained the phenotype of differentiated MSCs and the labeled MSCs-scaffold structure formed neocartilage *in vivo* (Fig. 9). In addition, these experiments demonstrated that the cells in the implants were derived from the chondrogenic induced MSCs.

Stem cells therapy holds great promise for use in tissue engineering application. To date, MSCs have been shown to be a unique stem cell for cartilage regeneration [32,33]. After the MSCs are harvested and expanded in culture, they can be combined with a scaffold for repair of cartilage defects. Moreover, the development of scaffolds is a fundamental component for MSCs-based cartilage tissue engineering applications. In this study, the scaffold walls, which entrapped more MSCs in the ACECM meshwork, were used to set up the oriented system. Moreover, the oriented microtubules could improve the diffusion of nutrients and removal of waste; facilitate cell migration into the center part of the scaffold and direct cell alignment along the oriented structure. Thus, the biomimetic oriented ACECM scaffold could be better for functional integration upon implantation in cartilage defects. Evaluation of the efficacy of the MSCs-ACECM scaffold system in animal models of articular cartilage defects is currently underway.

5. Conclusion

In the present study, a nanofibrous ACECM was fabricated by combining physical pulverization with a chemical

decellularization procedure. The ACECM derived oriented scaffold was developed using an improved TIPS technique. The scaffold was a biomimetic of the biochemical composition and morphological structure of deep zone articular cartilage. The ACECM scaffold provided a microenvironment for MSCs adherence and proliferation *in vitro*. In addition, PKH26 fluorescent labeled MSCs were observed in nude mice and the ability of MSCs chondrogenic differentiation *in vivo* was maintained in the scaffold. Thus, the oriented ACECM scaffold holds great promise for use in cartilage tissue engineering applications.

Acknowledgements

This study was funded by the National Natural Science Foundation of China (30973047), National High-Tech Research and Development Program (2007AA021902), National Science and Technology Supportive Program (2006BAI16B04).

References

1. Hunziker, E. B. (2002) Articular cartilage repair: Basic science and clinical progress. A review of the current status and prospects. *Osteoarthr. Cartilage.* 10: 432-463.
2. Gobbi, A., P. Nunag, and K. Malinowski (2005) Treatment of full thickness chondral lesions of the knee with microfracture in a group of athletes. *Knee Surg. Sports Traumatol. Arthrosc.* 13: 213-221.
3. Raghunath, J., H. J. Salacinski, K. M. Sales, P. E. Butler, and A. M. Seifalian (2005) Advancing cartilage tissue engineering: The application of stem cell technology. *Curr. Opin. Biotech.* 16: 503-509.
4. Sittinger, M., D. Reitzel, M. Dauner, H. Hierlemann, C. Hammer, E. Kastenbauer, H. Planck, G. R. Burmester, and J. Bujia (1996) Resorbable polyesters in cartilage engineering: Afnity and biocompatibility of polymer ber structures to chondrocytes. *J. Biomed. Mater. Res.* 33: 57-63.
5. Uematsu, K., K. Hattori, Y. Ishimoto, J. Yamauchi, T. Habata, Y. Takakura, H. Ohgushi, T. Fukuchi, and M. Sato (2005) Cartilage regeneration using mesenchymal stem cells and a three-dimensional poly lactic-glycolic acid (PLGA) scaffold. *Biomat.* 26: 4273-4279.
6. Yoo, H. S., E. A. Lee, J. J. Yoon, and T. G. Park (2005) Hyaluronic acid modied biodegradable scaffolds for cartilage tissue engineering. *Biomat.* 26: 1925-1933.
7. Sims, C. D., P. E. Butler, Y. L. Cao, R. Casanova, M. A. Randolph, A. Black, C. A. Vacanti, and M. J. Yaremchuk (1998) Tissue engineered neocartilage using plasma derived polymer substrates and chondrocytes. *Plast. Reconstr. Surg.* 101: 1580-1585.
8. Ting, V., C. D. Sims, L. E. Brecht, J. G. McCarthy, A. K. Kasabian, P. R. Connelly, J. Elisseeff, G. K. Gittes, and M. T. Longaker (1998) *In vitro* prefabrication of human cartilage shapes using fibrin glue and human chondrocytes. *Ann. Plast. Surg.* 40: 413-421.
9. Gong, Y. H., Q. L. Zhou, C. Y. Gao, and J. Shen (2007) *In vitro* and *in vivo* degradability and cytocompatibility of poly (L-lactic acid) scaffold fabricated by a gelatin particle leaching method. *Acta. Biomater.* 3: 531-540.
10. Alvarez-Barreto, J. F. and V. I. Sikavitsas (2007) Improved mesenchymal stem cell seeding on RGD- modied poly(L-lactic acid) scffolds using ow perfusion. *Macromol. Biosci.* 7: 579-588.
11. Sato, T., G. P. Chen, and T. Ushida (2001) Tissue engineered cartilage by *in vivo* culturing of chondrocytes in PLGA-collagen hybrid sponge. *Mater. Sci. Eng. C.* 17: 83-89.
12. Exposito, J. Y., M. D'Alessio, M. Solursh, and F. Ramirez (1992) Sea urchin collagen evolutionarily homologous to vertebrate pro-alpha 2(I) collagen. *J. Biol. Chem.* 267: 15559-15562.
13. Schenke-Layland, K., O. Vasilevski, F. Opitz, K. König, I. Riemann, K. J. Halbhuber, T. Wahlers, and U. A. Stock (2003) Impact of decellularization ofxenogeneic tissue on extracellular matrix integrity for tissue engineering of heart valves. *J. Struct. Biol.* 143: 201-208.
14. Conklin, B. S., E. R. Richter, K. L. Kreutziger, D. S. Zhong, and C. Chen (2002) Development and evaluation of anovel decellularized vascular xenograft. *Med. Eng. Phys.* 24: 173-183.
15. Chen, R. N., H. O. Ho, Y. T. Tsai, and M. T. Sheu (2004) Process development of an acellular dermal Matrix (ADM) for biomedical applications. *Biomat.* 25: 2679-2686.
16. Hudson, T. W., S. Y. Liu, and C. E. Schmidt (2004) Engineering an improved acellular nerve graft *via* optimized chemical processing. *Tissue Eng.* 10: 1346-1358.
17. Lanfer, B., F. P. Seib, U. Freudenberg, D. Stamov, T. Bley, M. Bornhäuser, and C. Werner (2009) The growth and differentiation of mesenchymal stem and progenitor cells cultured on aligned collagen matrices. *Biomat.* 30: 5950-5958.
18. Lin, A. S., T. H. Barrows, S. H. Cartmell, and R. E. Guldberg (2003) Microarchitectural and mechanical characterization of oriented porous polymer scaffolds. *Biomaterials* 24: 481-489.
19. Lanfer, B., A. Hermann, M. Kirsch, U. Freudenberg, U. Reuner, C. Werner, and A. Storch (2010) Directed growth of adult human white matter stem cell-derived neurons on aligned fibrillar collagen. *Tissue Eng.* 16: 1103-1113.
20. Gilbert, T. W., T. L. Sellaro, and S. F. Badylak (2006) Decellularization of tissues and organs. *Biomat.* 27: 3675-3683.
21. Whitehead, M. A., D. Fan, P. Mukherjee, G. R. Akkaraju, L. T. Canham, and J. L. Coffer (2008) High porosity poly (epsilon-caprolactone)/mesoporous silicon scaffolds: Calcium phosphate deposition and biological response to bone precursor cells. *Tissue Eng: Part A.* 14: 195-206.
22. Yang, H. N., J. S. Park, K. Na, D. G. Woo, Y. D. Kwon, and K. H. Park (2009) The use of green uorescence gene (GFP)-modied rabbit mesenchymal stem cells (rMSCs) co-cultured with chondrocytes in hydrogel constructs to reveal the chondrogenesis of MSCs. *Biomat.* 30: 6374-6385.
23. Li, W. J., Y. J. Jiang, and R. S. Tuan (2006) Chondrocyte phenotype in engineered fibrous matrix is regulated by fiber size. *Tissue Eng.* 12: 1775-1785.
24. Huang, N. F., S. Patel, R. G. Thakar, J. Wu, B. S. Hsiao, B. Chu, R. J. Lee, and S. Li (2006) Myotube assembly on nanobrous and micropatterned polymers. *Nano. Lett.* 6: 537-542.
25. Kim, H. D., E. H. Bae, I. C. Kwon, R. R. Pal, J. D. Nam, and D. S. Lee (2004) Effect of PEG-PLLA di block copolymer on macroporous PLLA scaffolds by thermally induced phase separation. *Biomat.* 25: 2319-2329.
26. Wei, G. B. and P. X. Ma (2004) Structure and properties of nano-Hydroxyapatite/polymer composite scaffolds for bone tissue engineering. *Biomat.* 25: 4749-4757.
27. Ma, P. X. and R.Y. Zhang (2001) Microtubular architecture of biodegradable polymer scaffolds. *J. Biomed. Mater. Res.* 56: 469-477.
28. Murugan, R. and S. Ramakrishna (2007) Design strategies of tissue engineering scaffolds with controlled ber orientation. *Tissue*

Eng. 13: 1845-1866.
29. Meinel, A. J., K. E. Kubow, E. Klotzsch, M. Garcia-Fuentes, M. L. Smith, V. Vogel, H. P. Merkle, and L. Meinel (2009) Optimization strategies for electrospun silk broin tissue engineering scaffolds. *Biomaterials* 30: 3058-3067.
30. Chen, J., C. Wang, S. Lü, J. Wu, X. Guo, C. Duan, L. Dong, Y. Song, J. Zhang, D. Jing, L. Wu, J. Ding, and D. Li (2005) *In vivo* chondrogenesis of adult bone marrow derived autologous mesenchymal stem cells. *Cell Tissue Res.* 319: 429-438.
31. Kang, E. J., J. H. Byun, Y. J. Choi, G. H. Maeng, S. L. Lee, D. H. Kang, J. S. Lee, G. J. Rho, and B. W. Park (2010) *In vitro* and *in vivo* osteogenesis of porcine skin-derived mesenchymal stem cell-like cells with a demineralized bone and fibrin glue scaffold. *Tissue Eng: Part A* 16: 815-827.
32. Kuroda, R., K. Isada, T. Matsumoto, T. Akisue, H. Fujioka, K. Mizuno, H. Ohgushi, S. Wakitani, and M. Kurosaka (2007) Treatment of a full-thickness articular cartilage defect in the femoral condyle of an athlete with autologous bone marrow stromal cells. *Osteoarthr. Cartilage* 15: 226-231.
33. Wakitani, S., K. Imoto, T. Yamamoto, M. Saito, N. Murata, and M. Yoneda (2002) Human autologous culture expanded bone marrow mesenchymal cell transplantation for repair of cartilage defects in osteoarthritic knees. *Osteoarthr. Cartilage* 10: 199-206.